Electrodeposition of Titanium in Water-soluble KF–KCl Molten Salt

Norikawa, Yutaro; Nohira, Toshiyuki; Yasuda, Kouji

Materials Transactions, Vol. 58, No. 3 (2017) pp. 390 to 394
Special Issue on New Proposals on Titanium Production and Molten Salts

Electrodeposition of Titanium in a Water-Soluble KF–KCl Molten Salt

Yutaro Norikawa[1,*1], Kouji Yasuda[2,3] and Toshiyuki Nohira[1,*2]

[1]*Institute of Advanced Energy, Kyoto University, Uji 611–0011, Japan*
[2]*Agency for Health, Safety and Environment, Kyoto University, Kyoto 606–8501, Japan*
[3]*Department of Fundamental Energy Science, Graduate School of Energy Science, Kyoto University, Kyoto 606–8501, Japan*

A new method of electrodeposition of Ti using a water-soluble KF–KCl molten salt electrolyte has been proposed. The electrochemical behaviors of Ti(III) ions in a KF–KCl molten salt to which 0.1 mol% K_2TiF_6 and an excess amount of sponge Ti were added have been investigated by cyclic voltammetry at 923 K. Anodic currents corresponding to the oxidation of Ti(III) ions were observed from 1.5 V (vs. K^+/K) at a glass-like carbon rod electrode. In the negative potential region, cathodic currents were seen from 0.3 V, indicating the deposition of Ti metal from Ti(III) ions. When a nickel flag electrode was used, cathodic currents due to the formation of Ti–Ni alloys were observed, in addition to the current of deposition of Ti metal. The analyses of the electrodeposits by scanning electron microscopy, energy dispersive X-ray spectroscopy, and X-ray diffractometry confirmed that dense and smooth films of Ti metal with 20 μm thickness were obtained at current densities of 2.5×10^{-2}–1.0×10^{-1} Acm^{-2}. [doi:10.2320/matertrans.MK201605]

(Received August 30, 2016; Accepted November 14, 2016; Published December 16, 2016)

Keywords: *titanium, molten salt, electrodeposition, fluoride–chloride*

1. Introduction

Titanium metal is widely utilized in the manufacture of airplane parts, industrial plants, biological implants etc. due to its superior properties such as high strength to weight ratio, corrosion resistance, heat resistance, and biocompatibility. Currently, titanium products are mainly manufactured by a two-step process. First, the titanium metal is produced by the Kroll process, in which Mg is used to reduce titanium tetrachloride. Next, the machining processes of the bulk titanium metal such as rolling and cutting are carried out. However, the current production method has several drawbacks such as high production cost for the Kroll process and the poor workability of titanium, which inhibit the widespread use of titanium. Therefore, the development of a new manufacturing process for titanium is required.

Toward this end, plating metallic titanium on general substrates is a promising approach to utilize the superior properties of titanium. For example, physical vapor deposition (PVD), which can produce high quality films, has been practically used in the semiconductor field. However, the deposition rate is extremely low, resulting in a high process cost, and the plating of substrates with complicated shapes is difficult.

Electrodeposition is the plating method of choice for titanium because of its potentially high deposition rate and low cost. Furthermore, plating substrates with complicated shapes is possible by electrodeposition. The electrodeposition of titanium metal has been studied in high-temperature molten salts. In previous studies, chloride melts[1–5], fluoride melts[6–13], and mixed fluoride–chloride melts[14–17] were investigated as electrolytes. In chloride melts such as LiCl–KCl[1], NaCl–KCl[2], $CaCl_2$[3], and NaCl–CsCl[4], the morphologies of the products were dendritic or rough surface. It has also been reported that the obtained deposit in molten NaCl[5] was not metallic Ti but a Ti–Fe alloy. In general, it is difficult to obtain smooth and compact films in chloride melts because three ionic species with different valence numbers, i.e., Ti(II), Ti(III), and Ti(IV), exist and undergo disproportionation reactions. However, compact and smooth Ti films were obtained in LiF–NaF–KF melts by Lepinay *et al.* at 823–1023 K[6] and by Robin *et al.* at 873–923 K[7–9]. The electrochemical reduction mechanism of Ti ions in molten LiF–NaF–KF and LiF–KF at 823–1023 K[10–13] was also studied. In these papers, Ti(III) and Ti(IV) ions were shown to achieve high stability by forming titanium–fluoro complex ions, and the deposition of Ti metal occurred in two steps by the reduction of Ti(IV) ions. Moreover, good deposits were obtained when the valence of the Ti ions was adjusted to be only Ti(III). In mixed fluoride–chloride melts, Oki *et al.* obtained compact smooth films in KCl–NaCl–LiCl containing K_2TiF_6 at 723–923 K[14,15], while Malyshev *et al.* reported similar results in KCl–NaCl–NaF–$TiCl_3$ at 1073 K[16]. The influence of the addition of F^- ions into chloride melts on the morphology of the Ti deposits has also been investigated. Song *et al.* reported that the addition of KF into KCl–NaCl up to a molar ratio of $[F^-]/[Ti^{n+}] = 6$ led to the deposition of Ti metal with fine crystal grains, which is advantageous for the formation of compact and smooth Ti films[17]. According to Oki *et al.*, Ti(II) ions were not formed during the electrochemical reduction when the added amount of KF in NaCl–KCl–3 mass% K_2TiF_6 exceeded 10 mass%[18]. To summarize, compact and smooth films are obtained in fluoride-based melts. However, the main disadvantage of these melts is the difficulty to remove the solidified salt from the obtained Ti films by water washing, because of the low solubility of fluoride salts (LiF; 0.13, NaF; 4.15, MgF_2; 0.13, CaF_2; 0.016 g per 100 g H_2O)[19].

Hence, we propose a new process for the electrodeposition of Ti using KF–KCl as a molten salt electrolyte. Fluoride-based molten salts are known to yield smooth and compact Ti films. Among the alkali and alkaline earth fluorides, KF has an exceptionally high solubility in water (101.6 g per 100 g H_2O)[19]. However, the use of KF molten salt is problematic, owing to the high melting point of KF (1131 K). Since KCl also has high a solubility in water (35.9 g per 100 g H_2O)[19], it is possible to lower the melting point by using a

*1Graduate Student, Kyoto University
*2Corresponding author, E-mail: nohira.toshiyuki.8r@kyoto-u.ac.jp

KF–KCl binary melt (melting point = 878 K at the eutectic composition[20]) without losing the water-solubility. Althogh LiCl, NaCl, $MgCl_2$, and $CaCl_2$ are also highly soluble in water, they form water-insoluble fluoride salts when they are added to molten KF. For example, LiF is produced according to the reaction, KF + LiCl → LiF + KCl. In a previous study by our group[21], compact and smooth Si films were electrodeposited in KF–KCl–K_2SiF_6 and the solidified salt was easily removed by water washing alone.

In the present paper, the electrochemical behavior of Ti(III) ions was investigated in the KF–KCl eutectic melt at 923 K. On the basis of previous studies[6–9,14–16], Ti(III) ions were obtained by the comproportionation reaction (1).

$$\mathrm{Ti(0) + 3Ti(IV) \rightarrow 4Ti(III)} \quad (1)$$

Specifically, K_2TiF_6 and an excess amount of sponge Ti were added to a KF–KCl melt. Then, the deposited samples were obtained by galvanostatic electrolysis at several current densities and analyzed by scanning electron microscopy (SEM), energy dispersive X-ray spectroscopy (EDX), and X-ray diffraction (XRD) to find the optimum current density conditions for the deposition of dense and compact titanium films.

2. Experimental Procedure

A schematic representation of the experimental apparatus is shown in Fig. 1. Reagent grade KF (Wako Pure Chemical Co., Ltd., > 99.0%) and KCl (Wako Pure Chemical Co., Ltd., > 99.5%) were mixed to achieve the eutectic composition (molar ratio of KF:KCl = 45:55, melting point = 878 K[20], 400 g) and loaded in a graphite crucible (Toyo Tanso Co., Ltd., outer diameter: 90 mm, inner diameter: 80 mm, and height: 120 mm) or nickel crucible (Chiyoda Industry Co., Ltd., outer diameter: 96 mm, and height: 102 mm). The mixture in the crucible was first dried under vacuum at 453 K for 72 h. The crucible was placed at the bottom of a stainless steel vessel in an air-tight Kanthal container and further dried under vacuum at 773 K for 24 h. The electrochemical measurements were conducted in a dry Ar atmosphere at 923 K in a glove box. After blank measurements in KF–KCl, 0.1 mol% K_2TiF_6 (Morita Chemical Industry Co., Ltd., > 97.5%) and an excess amount (10 g) of sponge Ti (Wako Pure Chemical Co., Ltd., > 99%) were added to the melt. Here, 10 g of sponge Ti is approximately 100 times the amount necessary to generate Ti(III) ions from 0.1 mol% K_2TiF_6 according to eq. (1).

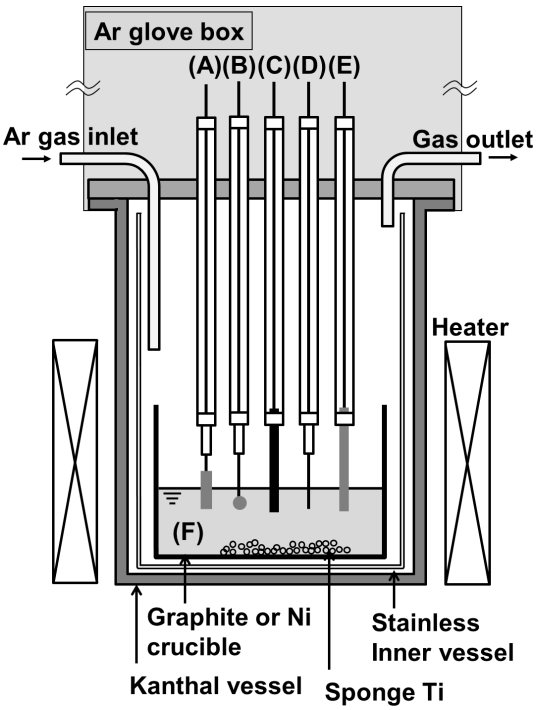

Fig. 1 A schematic representation of the experimental apparatus: (A) Ni plate electrode, (B) Ni flag electrode, (C) glass-like carbon rod electrode, (D) Pt and Mo wire electrodes, (E) Ti rod electrode, and (F) molten KF–KCl.

Electrochemical measurements and galvanostatic electrolysis were conducted using a three-electrode system (Hokuto Denko Corp., HZ-3000). The working electrodes were a Ni plate (Nilaco Corp., 5 mm × 10 mm, thickness: 0.1 mm, > 99%), a Ni flag (Nilaco Corp., diameter: 2.0 mm, thickness: 0.1 mm, 99.98%), and a glass-like carbon (G.C.) rod (Tokai Carbon Co., Ltd., diameter: 3.0 mm). The structure of the Ni flag electrode was reported in our previous paper[21]. In order to remove the oxide film before usage, a Ni plate for electrodeposition was electropolished in 50 mass% sulfuric acid at 200 $mAcm^{-2}$ for 10 s, dipped in aqueous solution containing sodium bifluoride, and followed by washing in hydrochloric acid of pH = 4.0, at room temperature. The Ni plate was then washed by ethanol and dried. A Ti rod (Nilaco Corp., diameter: 3.0 mm, 99.5%) was used as the counter electrode, and a Pt wire (Nilaco Corp., diameter: 1.0 mm, > 99.98%) was employed as a quasi-reference electrode. The potential of the reference electrode was calibrated with reference to a dynamic K^+/K potential estimated by cyclic voltammetry on a Mo wire (Nilaco Corp., diameter: 1.0 mm, 99.95%). The temperature of the melt was measured by a type K thermocouple. The electrolyzed samples on the Ni plates were soaked in distilled water at 333 K for 1 h to remove the salt adhered on the deposits. The cross-sections of the samples were studied by SEM (Keyence Corp., VE-8800). For the observation, the samples were embedded in acrylic resin and polished with emery papers and buffing compounds. After polishing, the samples were coated with Au by an ion sputtering apparatus (Hitachi, Ltd., E-1010) to give conductivity. The deposits were also characterized by EDX (AMETEK Co., Ltd., EDAX Genesis APEX2) and XRD (Rigaku Corp., Ultima IV, Cu-$K\alpha$ line).

3. Results and Discussion

3.1 Cyclic voltammetry

Figure 2(A) shows the cyclic voltammograms from the open-circuit potential to the positive direction measured at a glass-like carbon electrode before and after the addition of 0.1 mol% K_2TiF_6 and an excess amount of sponge Ti at 923 K. The anodic currents sharply increase at 3.6 V (vs. K^+/K) (current (b)) before and after the addition. The theoretical decomposition voltage of KCl(l) is calculated to be 3.63 V from the standard Gibbs energy of formation (-345.516 kJ mol^{-1})[22], assuming that the activity of Cl^- ions follows Raoult's law. Thus, it is conceivable that the anodic currents above 3.6 V correspond to the generation of Cl_2 gas.

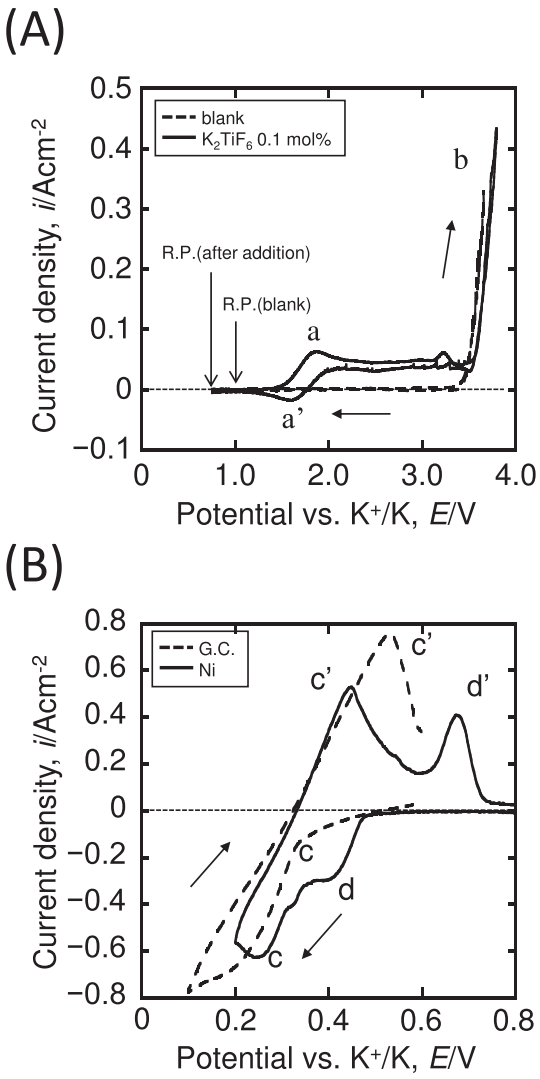

Fig. 2 Cyclic voltammograms in molten KF–KCl at 923 K obtained at a scan rate of 0.10 Vs^{-1}. (A) Positive potential region was measured with a glass-like carbon rod electrode before (dashed curve) and after (solid curve) the addition of 0.1 mol% K_2TiF_6 and an excess amount of sponge Ti. (B) Negative potential region was measured with a glass-like carbon rod electrode (dashed curve) and a Ni flag electrode (solid curve) after the addition of 0.1 mol% K_2TiF_6 and an excess amount of sponge Ti.

$$2Cl^- \rightarrow Cl_2(g) + 2e^- \quad (2)$$

After the addition of K_2TiF_6 and sponge Ti, anodic currents are also observed from 1.5 V on the positive scan (current (a)), which is explained by the oxidation of Ti(III) to Ti(IV)[7].

$$Ti(III) \rightarrow Ti(IV) + e^- \quad (3)$$

In the present experiment, the rest potential (R.P.) was observed at approximately 0.7 V. Since this value is much more negative than the redox potential of Ti(IV)/Ti(III), most of the Ti ions exist as Ti(III) in the melt.

Figure 2(B) shows the cyclic voltammograms measured at the glass-like carbon from 0.6 V to the negative direction (dashed curve) and Ni flag electrodes from 0.8 V to the negative direction (solid curve) after the addition of K_2TiF_6 and sponge Ti. For both electrodes, cathodic currents flow from approximately 0.3 V (current (c)). After the reversal of scanning direction, the corresponding anodic currents are also observed. From this result, it is expected that Ti metal is deposited from Ti(III) ions at potentials more negative than 0.3 V.

$$Ti(III) + 3e^- \rightarrow Ti(0) \quad (4)$$

At the nickel flag electrode in Fig. 2(B), reduction currents are also observed from 0.5 V (current (d)). From the phase diagram of the Ti–Ni system, three intermetallic compounds, $TiNi_3$, TiNi, and Ti_2Ni exist at 923 K[23]. Thus, the observed currents (d) are likely to be associated with the formation of these Ti–Ni alloys.

$$Ti(III) + Ni(s) + 3e^- \rightarrow Ti–Ni(s) \quad (5)$$

The corresponding anodic currents (d') are then explained by the dissolution of Ti from the alloys.

$$Ti–Ni(s) \rightarrow Ti(III) + Ni(s) + 3e^- \quad (6)$$

3.2 Galvanostatic electrolysis

To prepare the deposition samples, galvanostatic electrolysis was conducted using the Ni plate electrodes at 923 K. Figure 3 shows the surface and cross-sectional SEM images of samples. The current densities were (a) 2.5×10^{-2}, (b) 5.0×10^{-2}, (c) 1.0×10^{-1}, and (d) 1.5×10^{-1} Acm^{-2}. The total quantity of electricity was fixed at 150 C. As seen from the surface SEM images, the films prepared under conditions (a), (b), and (c) were densely packed with compact crystal grains. From the cross-sectional SEM images at the center of the sample plates, the films had smooth surfaces and thicknesses around 20 μm. EDX analysis revealed only Ti, implying that all the components of the molten salt electrolyte (K, F, and Cl) were below the detection limits. Thus, the adhered salt on the Ti deposit was successfully dissolved by water washing.

As seen in the XRD patterns (Fig. 4), deposition of crystalline titanium metal is confirmed for samples (a), (b), and (c). Thus, the reduction currents approximately at 0.3 V were due to the deposition of Ti metal. The current efficiencies for Ti deposition calculated from the weight increase were 87%, 77%, and 81% at 2.5×10^{-2}, 5.0×10^{-2}, and 1.0×10^{-1} Acm^{-2}, respectively. Under the assumption of a 3-electron reaction, the theoretical thickness of the Ti layer is calculated to be 55 μm, which is much higher than the observed thickness about 20 μm. This could be attributed to the uneven distribution of current – high current densities at the edges and low current densities at the center. Moreover, as shown in the high magnification SEM image of sample (b) (Fig. 5), Ti–Ni alloy layers with 3 μm thickness are observed at the interface between a deposited Ti film and a Ni substrate. Meanwhile, Ti films were not obtained at the highest current density of (d) 1.5×10^{-1} Acm^{-2}. This is explained by the deposition of a K metal fog at high current density and the detachment of the metal deposit. A similar phenomenon was observed for the deposition of Si in the KF–KCl molten salt[24].

The preferred crystal orientation of the obtained Ti films was evaluated from the peak intensities in the XRD patterns. Table 1 lists the orientation index α_{hkl} calculated for samples (a), (b), and (c) using the equation proposed by Willson *et al.*[25]

$$\alpha_{hkl} = \frac{I_{hkl}(sample)/\sum I(sample)}{I_{hkl}(PDF)/\sum I(PDF)} \quad (7)$$

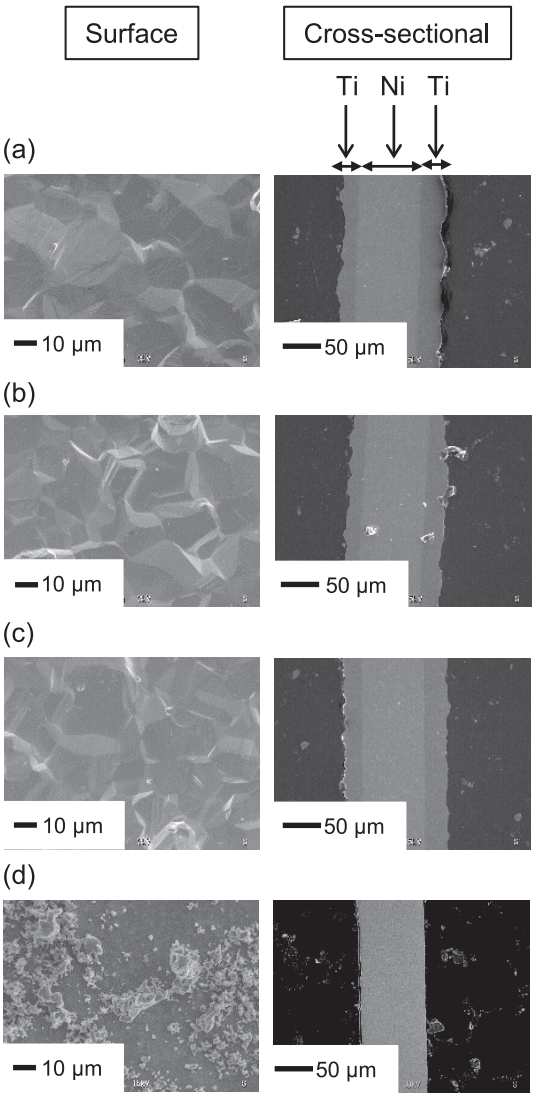

Fig. 3 Surface and cross-sectional SEM images of the samples obtained by galvanostatic electrolysis of Ni plate electrodes in molten KF–KCl after the addition of K_2TiF_6 (0.1 mol%) and an excess amount of sponge Ti at 923 K. Cathodic current density and time: (a) 2.5×10^{-2} Acm^{-2} for 100 min, (b) 5.0×10^{-2} Acm^{-2} for 50 min, (c) 1.0×10^{-1} Acm^{-2} for 25 min, and (d) 1.5×10^{-1} Acm^{-2} for 16.7 min.

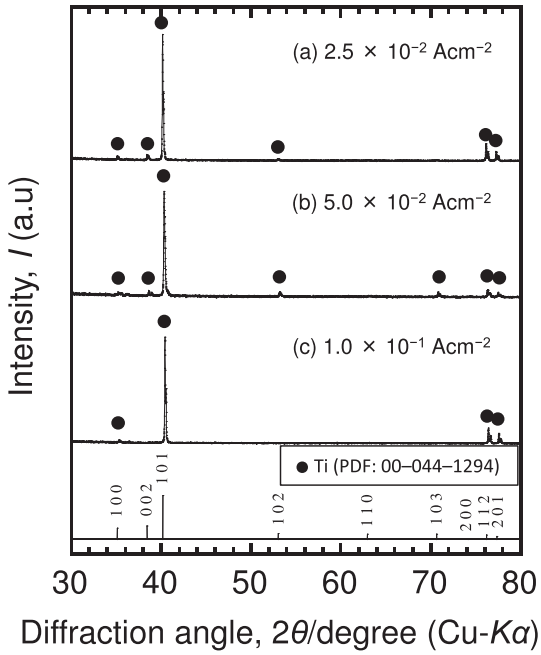

Fig. 4 XRD patterns of the samples obtained by galvanostatic electrolysis of Ni plate electrodes in molten KF–KCl after the addition of K_2TiF_6 (0.1 mol%) and an excess amount of sponge Ti at 923 K. Cathodic current density and time: (a) 2.5×10^{-2} Acm^{-2} for 100 min, (b) 5.0×10^{-2} Acm^{-2} for 50 min, and (c) 1.0×10^{-1} Acm^{-2} for 25 min.

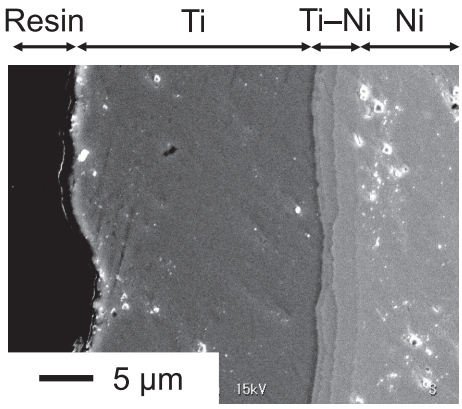

Fig. 5 A cross-sectional SEM image of the sample obtained by galvanostatic electrolysis of a Ni plate electrode in molten KF–KCl after the addition of K_2TiF_6 (0.1 mol%) and an excess amount of sponge Ti at 923 K. Cathodic current density and time: 5.0×10^{-2} Acm^{-2} for 50 min.

Here, $I_{h\,k\,l}$(sample) and $I_{h\,k\,l}$(PDF) indicate the peak intensity of $h\,k\,l$ plane for the deposits and PDF data (# 00–044–1294), respectively. The values of $\sum I$(sample) and $\sum I$(PDF) indicate the sum of peak intensities for the all planes for the deposits and PDF data, respectively. As the result, $\alpha_{1\,0\,1}$ is higher than 1.8 for all the deposits, which demonstrates the high orientation to 101 plane. Oki *et al.* reported that the Ti metal film deposited on nickel in KCl–NaCl–LiCl containing K_2TiF_6 at 923 K was highly orientated to 002 plane[17]. They also reported that the orientation varied with temperature, electrolysis time, current density, and electrolysis method. Similarly, the preferred orientation might be influenced by the electrolysis conditions in the present case, and will be reported in the future.

4. Conclusions

Electrodeposition of titanium metal was investigated in a KF–KCl molten salt containing Ti(III) ions at 923 K. The Ti(III) ions were prepared by the addition of 0.1 mol% K_2TiF_6 and an excess amount of sponge Ti, and the electrochemical behaviors were investigated by cyclic voltammetry. The oxidation of Ti(III) ions to Ti(IV) ions was observed from 1.5 V (vs. K^+/K) in the positive scan at a glass-like carbon electrode. Cathodic currents corresponding to the deposition of metallic Ti were observed at potentials more negative than 0.3 V. The solidified salt was successfully removed by washing with water, and the deposits obtained by galvanostatic electrolysis were analyzed by surface and cross-sectional SEM, EDX, and XRD. The films deposited at current densities of 2.5×10^{-2}–1.0×10^{-1} Acm^{-2} had smooth surfaces and approximately 20 μm thickness. XRD analysis revealed that

Table 1 Orientation index of the samples obtained by galvanostatic electrolysis of Ni plate electrodes in molten KF–KCl after the addition of K_2TiF_6 (0.1 mol%) and an excess amount of sponge Ti at 923 K. Cathodic current density and time: (a) 2.5×10^{-2} Acm^{-2} for 100 min, (b) 5.0×10^{-2} Acm^{-2} for 50 min, and (c) 1.0×10^{-1} Acm^{-2} for 25 min.

Plane, $h\,k\,l$	Diffraction angle, 2θ/degree (Cu-$K\alpha$)	Orientation index, $\alpha_{h\,k\,l}$		
		2.5×10^{-2} Acm^{-2}	5.0×10^{-2} Acm^{-2}	1.0×10^{-1} Acm^{-2}
1 0 0	35.09	0.12	0.07	0.12
0 0 2	38.42	0.31	0.38	0.00
1 0 1	40.17	1.86	1.88	1.92
1 0 2	53.01	0.13	0.42	0.00
1 1 0	62.95	0.04	0.06	0.00
1 0 3	70.66	0.00	0.52	0.00
2 0 0	74.15	0.00	0.00	0.00
1 1 2	76.22	1.53	0.91	1.64
2 0 1	77.37	1.06	0.59	1.28

crystalline metallic titanium was deposited, and that the titanium films were highly orientated to 101 plane.

Acknowledgment

A part of this study was conducted as collaborative research with Sumitomo Electric Industries, Ltd.

REFERENCES

1) G.M. Haaberg, W. Rolland, A. Sterten and J. Thonstad: J. Appl. Electrochem. **23** (1993) 217–224.
2) X. Ning, H. Asheim, H. Ren, S. Jiao and H. Zhu: Metall. Mater. Trans., B **42** (2011) 1181–1187.
3) M.H. Kang, J. Song, H. Zhu and S. Jiao: Metall. Mater. Trans., B **46** (2015) 162–168.
4) Y. Song, S. Jiao, L. Hu and Z. Guo: Metall. Mater. Trans., B **47** (2016) 804–810.
5) T. Uda, T.H. Okabe, Y. Waseda and Y. Awakura: Sci. Technol. Adv. Mater. **7** (2006) 490–495.
6) J. de Lepinay, J. Bouteillon, S. Traore, D. Renaud and M.J. Barbier: J. Appl. Electrochem. **17** (1987) 294–302.
7) A. Robin, J.D. Lepinay and M.J. Barbier: J. Electroanal. Chem. **230** (1987) 125–141.
8) A. Robin: Mater. Lett. **34** (1998) 196–201.
9) A. Robin and R.B. Ribeiro: J. Appl. Electrochem. **30** (2000) 239–246.
10) J. O'M. Bockris, G.J. Hills, I.A. Menzies and L. Young: Nature **178** (1956) 654.
11) F.R. Clayton, G. Mamantov and D.L. Manning: J. Electrochem. Soc. **120** (1973) 1193–1198.
12) J. de Lepinay and P. Paillere: Electrochim. Acta **29** (1984) 1243–1250.
13) A. Girginov, T.Z. Tzvetkoff and M. Bojinov: J. Appl. Electrochem. **25** (1995) 993–1003.
14) D. Wei, T. Tada and T. Oki: ISIJ Int. **33** (1993) 1016–1022.
15) D. Wei, M. Okido and T. Oki: J. Appl. Electrochem. **24** (1994) 923–929.
16) V.V. Malyshev and D.B. Shakhnin: Mater. Sci. **50** (2014) 80–91.
17) J. Song, Q. Wang, X. Zhu, J. Hou, S. Jiao and H. Zhu: Mater. Trans. **55** (2014) 1299–1303.
18) C. Guang-Sen, M. Okido and T. Oki: J. Appl. Electrochem. **18** (1988) 80–85.
19) R. Kubo, S. Nagakura, H. Iguchi and H. Ezawa: Rikagaku Jiten, 4th Edition, Iwanami Shoten, Tokyo (1987).
20) L. P. Cook and H. F. McMurdie: Phase Diagrams for Ceramists vol. VII, The American Ceramic Society Inc., Ohio (1989) 509.
21) K. Maeda, K. Yasuda, T. Nohira, R. Hagiwara and T. Homma: J. Electrochem. Soc. **162** (2015) D444–D448.
22) M.W. Chase, Jr., C.A. Davies, J.R. Downey, Jr., D.L. Frurlp, R.A. Macdonald and A.N. Syverud: J. Phys. Chem. Ref. Data **14** Suppl. 1 (1985) 754.
23) H. Okamoto: J. Phase Equilib. **36** (2015) 390–401.
24) K. Yasuda, K. Maeda, T. Nohira, R. Hagiwara and T. Homma: J. Electrochem. Soc. **163** (2016) D95–D99.
25) K.S. Willson and J.A. Rogers: Tech. Proc. Amer. Electroplaters Soc. **51** (1964) 92–95.